What You Can't Feel Won't Hurt You: Evaluating Haptic Hardware Using a Haptic Contrast Sensitivity Function

Curt M. Salisbury, R. Brent Gillespie, *Member*, *IEEE*, Hong Z. Tan, *Senior Member*, *IEEE*, Federico Barbagli, and J. Kenneth Salisbury, *Member*, *IEEE*

Abstract—In this paper, we extend the concept of the contrast sensitivity function—used to evaluate video projectors—to the evaluation of haptic devices. We propose using human observers to determine if vibrations rendered using a given haptic device are accompanied by artifacts detectable to humans. This determination produces a performance measure that carries particular relevance to applications involving texture rendering. For cases in which a device produces detectable artifacts, we have developed a protocol that localizes deficiencies in device design and/or hardware implementation. In this paper, we present results from human vibration detection experiments carried out using three commercial haptic devices and one high performance voice coil motor. We found that all three commercial devices produced perceptible artifacts when rendering vibrations near human detection thresholds. Our protocol allowed us to pinpoint the deficiencies, however, and we were able to show that minor modifications to the haptic hardware were sufficient to make these devices well suited for rendering vibrations, and by extension, the vibratory components of textures. We generalize our findings to provide quantitative design guidelines that ensure the ability of haptic devices to proficiently render the vibratory components of textures.

Index Terms—Haptics, design, psychophysics, texture, evaluation of haptic devices, haptic contrast sensitivity function (HCSF).

1 Introduction

With the plethora of haptic devices that are commercially available today, the question often arises: what device is "good enough" for a given application? While a haptic device may come with specifications for its mechanical and electrical properties, no clear relationship between these properties and application-specific performance is available from the commercial or academic literature. The goal of the present study is to bridge this gap by evaluating haptic hardware in the context of a given application involving human users.

In developing our approach, we note that a similar issue has already been addressed in the use of optical instruments such as telescopes and projectors that display to the eye. Mouroulis [2] determined that a telescope is "good enough" so long as the visual artifacts generated by optical defects are not detectable by human observers. To determine the presence of detectable artifacts, sinusoidal gratings were presented through the telescope to human observers and detection threshold experiments were conducted. From these threshold data, a Contrast Sensitivity Function (CSF) was generated, which is the inverse of the sinusoidal grating detection threshold, reported as a function of spatial frequencies in cycles per degree of visual angle. Now, the use of sinusoidal gratings to generate a CSF from human participant tests was already a standard technique for characterizing human perception. Human perception in terms of the CSF was found to be consistent across normal observers. Using the same test protocol to characterize the hardware, however, was a novel concept. In a way, the human became the measurement instrument and the hardware became the participant. Specifically, the CSFs generated with given hardware were then compared to the CSFs found in the literature. Deviations from the CSFs limited only by human perception would indicate the presence of hardware inadequacies that were detectable to human observers. Tying hardware evaluations to human perception in this way has the distinct advantage of indicating when the hardware is "good enough" for human use. The use of CSF to evaluate hardware has since been applied to the calibration of video projectors. The CSF has also recently been incorporated into control algorithms that reduce banding in hardcopy images produced by inkjet printers [3].

Can the concept of applying a psychophysical test protocol such as CSF to the evaluation of hardware be applied to the evaluation of haptic devices in which the human is used as the measurement instrument? If so, what

- *C.M. Salisbury is with the Intelligent Systems, Robotics, and Cybernetics Group at Sandia National Laboratories, 1515 Eubank SE, BLDG 895 RM 2263, Albuquerque, NM, 87123. E-mail: cmsalis@sandia.gov.*
- *R.B. Gillespie is with the Haptix Laboratory, University of Michigan, 2350 Hayward St., Ann Arbor, MI 48109. E-mail: brentg@umich.edu.*
- *H.Z. Tan is with the Haptic Interface Research Laboratory, Purdue University, 465 Northwestern Avenue, West Lafayette, IN 47907. E-mail: hongtan@purdue.edu.*
- *F. Barbagli is with the Department of Computer Science, Stanford University, 353 Serra Mall, Stanford, CA 94305-9025. E-mail: fedster@gmail.com.*
- *J.K. Salisbury is with the BioRobotics Laboratory, Stanford University, 318 Campus Drive, E1.3 E100 BioRobotics, Stanford, CA 93405. E-mail: jks@robotics.stanford.edu.*

Manuscript received 2 July 2009; revised 5 Feb. 2010; accepted 23 Nov. 2010; published online 25 Feb. 2011.
Recommended for acceptance by A. Kappers.
For information on obtaining reprints of this article, please send e-mail to: toh@computer.org, and reference IEEECS Log Number TH-2009-07-0044.
Digital Object Identifier no. 10.1109/ToH.2011.5.

is the haptic equivalent of CSF? Just as the visual CSF is derived from psychophysical detection thresholds of visual spatial sinusoidal gratings, we propose a haptic CSF which is derived from psychophysical detection thresholds of temporal sinusoidal displacements. If we plot the inverse of vibration detection thresholds as a function of temporal frequency, we have the haptic contrast sensitivity function (HCSF). Much like the visual detection thresholds of visual spatial sinusoidal gratings, detection thresholds in terms of vibrational displacements have been well established in the literature [4], [5]. We propose to use normal human observers along with the understanding of human detection thresholds to characterize haptic hardware. To do this, we use the same protocol used in psychophysical measurement of detection thresholds, but with commercial haptic hardware instead of standard laboratory testing equipment such as a minishaker. We point out that these experiments will require us to analyze the results differently than we would for a normal detection threshold experiment.

While a minishaker is calibrated and controlled so that the proximal stimuli are perfectly sinusoidal at the desired peak-to-peak displacement amplitude, we do not calibrate or control the proximal stimuli generated by the commercial haptic hardware used in our experiments. Instead, we command a sinusoidal force vibration in software and accept the resultant proximal stimuli. If the commercial device is perfectly linear and free of background noise, then commanding a sinusoidal force in software would result in a proximal stimulus which is a sinusoidal displacement vibration at the same frequency. If the device is not linear or is plagued with background noise, then the proximal stimuli due to forces commanded in software will be plagued with artifacts. In this case, we would not expect a straightforward relationship between forces commanded in software and proximal stimuli.

Because the experimental protocol we propose is forced choice, the participants are instructed to select which of three presented stimuli is unique (two of which are null stimuli). If the hardware presenting the proximal stimuli is "good enough," then the only cue in the proximal stimuli that the participant can use to identify the unique stimulus should be the sinusoidal displacement vibration at the same frequency as the sinusoidal force vibration commanded in software, and the detectable amplitudes (detection thresholds) of these sinusoidal displacement vibrations should match what is published in the literature. If the hardware presenting the proximal stimuli is deficient, however, then the proximal stimulus will not be a single frequency sinusoid and describing the results of these experiments as detection thresholds does not make sense. Instead, we propose to describe the results of the experiments more generally—in terms of the smallest distinguishable proximal stimuli, regardless of its spectral composition. Consider haptic hardware that is deficient in that, in addition to a single frequency sinusoid at the frequency of the force sinusoid commanded in software, it generates background noise (present in all three stimuli) near or about the same frequency. We would expect participants to be unable to distinguish between null and normally distinguishable sinusoidal stimuli due to masking effects. As a result, the amplitudes of the distinguishable sinusoids would be higher than those published in the literature. Careful analysis of the smallest distinguishable proximal stimuli will enable us to identify such a hardware deficiency. Another indication of hardware deficiency would be a proximal stimulus with several spectral components, whose amplitude and frequency are related in a nonlinear fashion to the sinusoidal force commanded in software. Earlier work showed that the smallest distinguishable proximal stimulus in which the proximal stimulus is a multispectral sinusoid is predicted by the smallest signal for which at least one spectral component was at the detection threshold for the associated frequency [6]. Again, careful analysis of the smallest distinguishable proximal stimuli will enable us to identify such a hardware deficiency.

This proposed test protocol is appealing because it not only links hardware performance to human perception, but it also links hardware performance to a specific application, namely texture rendering. While vibration plays a lesser role in the perception of surface textures with interelement spacing above 1 mm when using the bare fingertip, it plays a crucial role when using a rigid link interposed between the bare fingertip and the textured surface, regardless of interelement spacing [7], [8], [9], [10], [11], [12], [13], [14]. Katz was perhaps the first to demonstrate the importance of vibrations in conveying texture information by rubbing a pencil against coarse writing paper. He demonstrated impaired texture perception when the tip of the pencil was wrapped in cloth [15]. In order for point-contact force-feedback haptic devices to adequately render virtual textures, they must faithfully reproduce the relevant vibrations at the interface with the human skin. Furthermore, the presence of additional signals or artifacts in the proximal stimuli may affect human perception if they exceed the human detection thresholds, potentially causing the textures to feel unrealistic. On the other hand, haptic hardware could be deemed "good enough" at rendering the vibratory component of texture if the associated signal strengths do not exceed detection thresholds because these cues will not be perceptible to the human observer.

Others have explored using the human as a measurement instrument to guide the development of various system parameters. For example, MacLean linked device sampling, frequency, and damping to user perception [16]. Lawrence et al. proposed the use of rate-hardness as a perceptually relevant performance metric [17]. O'Malley and Goldfarb related peak continuous force to geometric size discrimination and identification [18]. In a series of studies investigating the effect of haptic system attributes on the perceived realism of virtual textures, Choi and Tan studied the effects of virtual stiffness value [19], rendering algorithm [20], and sampling rate [21] on the existence of realism-compromising instability. They found that low sampling rates, large stiffnesses, and a poor selection of rendering algorithms introduced unintended percepts. Some percepts could be attributed to buzzing that in turn could be associated with the existence of hardware structural resonances within the control loop. Others were attributed to sensory mechanisms, such as the mismatch of human sensitivities to displacement and force variations. They formulated guidelines for the sampling

rates, stiffness values, and rendering algorithms that would prevent the introduction of unintended percepts. Campion and Hayward analyzed the effect of electrical and mechanical characteristics of a haptic device on the proximal stimuli [22], but did not use human perception to qualify these effects.

We have extended the work of these researchers by using human observers to measure the effect of electrical and mechanical attributes of a haptic device on the perception of virtual textures. As pointed out above, because haptic devices must faithfully reproduce the relevant vibrations at the interface with the human skin in order to adequately render virtual textures, we use human vibration perception for our experiments. Our approach of conducting experiments on human participants using threshold detection protocol draws inspiration from the success of the CSF in characterizing visual displays such as projectors. Although thresholds and the CSF are simply related as the reciprocal of one another, we will report our results in terms of spectral displacement in dB relative to 1 micron because this is more commonly used in the haptics literature. In addition to characterizing the adequacy of various haptic hardware to render the vibratory components of realistic textures, the present study presents electrical and mechanical design guidelines for haptic hardware that will ensure such adequacy. By addressing certain hardware attributes with remedies and carrying out a threshold detection experiment a second time, we demonstrate the concrete relationship between these hardware attributes and the results of human perception experiments.

1.1 Overview of the Present Study

To develop the HCSF by applying the CSF concept to vibration detection, we used human participants and a detection experiment protocol to evaluate multiple haptic devices. We evaluated three commercially available haptic devices and a high-bandwidth linear voice-coil actuator with five participants. Our experiment used a one-up three-down adaptive method and the amplitude of the force sinusoid commanded in software was used as the independent variable. Again, we point out that this is a departure from the use of the displacement amplitude of vibrations of the proximal stimuli as the independent variable. In order to understand the smallest distinguishable proximal stimuli in terms of displacement, we measured the displacement signal post hoc with an accelerometer while driving the haptic device with the force sinusoid commanded in software that was identified in the experiments to generate the smallest distinguishable proximal stimuli. We then compared the displacement spectrum of these signals to the detection thresholds found in published literature [23]. A haptic device would be considered "good enough" for rendering the vibratory component of realistic textures if the smallest distinguishable proximal stimulus had a spectral component at the commanded frequency whose amplitude was at or near the detection thresholds found in the published literature, and the amplitude of every other spectral component was below the detection thresholds for the corresponding frequencies found in the published literature.

For those devices that were not "good enough," we examined time-series data measured post hoc to find clues as to which electrical and/or mechanical design attributes could be associated with the deficiencies. We show that the attributes that had the most detrimental effect on the adequacy of the haptic devices were nonlinearities including backdrive static friction, actuator signal quantization, and amplifier hysteresis. We then show that modifying or masking these limiting attributes enabled the devices to be "good enough." Finally, our work enables the suggestion of psychophysically-based design goals for device attributes that affect the perception of textures. We suggest the minimum force resolution as well as the maximum hysteresis, stiction, and backlash a device can possess, yet still be "good enough" for rendering the vibratory component of textures.

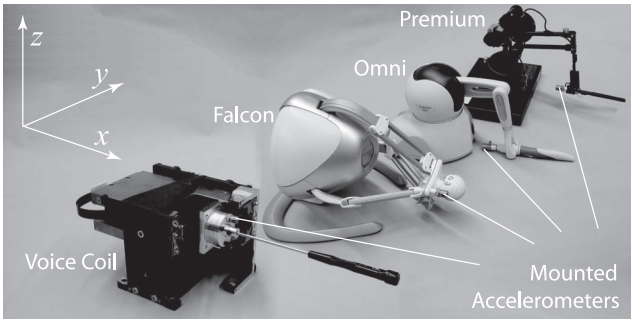

Fig. 1. Linear voice-coil actuator and haptic devices for experimental evaluation. (Modified from Fig. 1 in [1].)

2 Experiment 1

2.1 Methods

2.1.1 Apparatus

Three commercially available haptic devices were used in our study: the PHANTOM Premium 1.0, the PHANTOM Omni (both from Sensable Technologies, Woburn, MA), and the Falcon (Novint, Albuquerque, NM). These three devices are shown along with a linear voice coil actuator in Fig. 1. Each device, with the exception of the voice coil, was controlled through CHAI3d [24], a freeware platform that supports a variety of haptic devices.

A linear voice-coil actuator was used as a gold standard, supposing that the superior electrical and mechanical behavior would preclude it from generating artifacts in the proximal stimuli that would have an effect on the experiment. The voice coil was from an obsolete disk drive head actuator mechanism. It features coreless aluminum windings attached to an aluminum flange armature, all mounted on precision linear bearings. The mechanical dynamics of this system are dominated by a mass of 210 grams. The electrical inductance and resistance are 1.02 mH and 8.4 Ω, respectively. These properties result in a transfer function relating input voltage to output force (with the armature clamped) that is flat up to approximately 1 kHz, calibrated to be 1.456 N/V. We drove this device directly through the 16 bit digital-to-analog (D/A) converter of a National Instruments data acquisition board (National Instruments PCI-6259, Austin, TX) by commanding a reference voltage. The D/A of this board is capable of sourcing up to 5 mA. Because the currents required for our experiment were

below this level, an additional inline current amplifier was unnecessary.

All devices were run on a PC operating Windows XP. The three commercial devices ran at their native servo loop rates of 1 kHz. The voice coil was driven using a servo rate of ≈ 15 kHz with a jitter of approximately 9.2 μs on the period. This large jitter is actually due to a few outliers of large period.

Impedance type haptic devices operate by reading displacement x_h at the human-device interface and responding by commanding a force F_r in software, which in turn produces a force F_h on the hand. In this experiment, a sinusoidal force commanded in software $F_r(t) = A_r \sin(2\pi f t)$ was sent to each haptic device, where A_r was the amplitude of the sinusoid. As a function of the biomechanics of the finger pulp, finger, and hand, the applied force F_h gave rise to displacement x_h at the interface between hand and device. Displacement x_h was the proximal stimulus. The haptic devices in our experimental pool used encoders to measure position, but we found that their resolution was insufficient to resolve displacements for our purposes. Instead, we estimated displacements using an attached accelerometer. The accelerometer (model 8702B25, 200 mV/g, 1-8,000 Hz, Kistler Instrument Corp., Amherst, NY) provided good sensitivity to low values of acceleration. An accelerometer mount was added to each of the four devices (see Fig. 1). The mounts were attached as close as possible to the participant's hand to ensure that it measured what the fingers experienced. The mount and accelerometer weighed 2 and 8 grams, respectively. The accelerometer was sampled for all devices through the 16-bit Analog-to-Digital port on the NI board at 15 kHz.

2.1.2 Participants

Four males and one female (age 23-31 years old, average 26 years old) participated in the study. All were right handed by self-report. All participants (P1-P5) had interacted with haptic devices prior to this experiment.

2.1.3 Procedure

Each participant sat at a desk containing the haptic devices to be tested, a computer monitor, and a keyboard. They held each device interface (a ball-shaped interface for the Falcon, and a pen-shaped stylus for the other three devices; see Fig. 1) with their dominant hand. For the approximately 50 mm diameter spherical interface of the Falcon, they were instructed to hold it with a baseball-style grip. For the pen-like interfaces, they were asked to hold the stylus like a pen, parallel to the axis of motion. Prior experiments show the results of detection experiments for both interface types to be similar [23], [25]. Furthermore, prior research has shown that contact areas greater than 3.0 cm^2 produce similar results in detection experiments [26]. Because the contact areas of the sphere and pen are approx. 11 and 5.5 cm^2, respectively, we presume that results from each type can be directly compared. The axis of motion for each of the tested haptic devices was aligned to the x-axis as illustrated in Fig. 1. The participant's wrist and elbow were supported by foam pads to facilitate a natural posture and to minimize fatigue. Participants wore headphones playing white noise to mask auditory cues from the haptic devices.

Two test frequencies ($f = 40, 160$ Hz) were used to compare the smallest distinguishable proximal stimuli of the four devices. These frequencies were selected to facilitate direct comparison to thresholds and frequencies tested in the literature. We used a within-participant design, and the order of the frequencies and devices tested was randomized for each participant.[1] In each trial, the participant was presented with stimuli according to a three-interval, forced-choice, one-up three-down adaptive method [27]. Taking inspiration from the definition of experimental construction of the Contrast Sensitivity Function, we used vibration amplitude as the independent variable in our experiments. The vibrations rendered by the various devices to our participants may be described in terms of the history of displacement $x_h(t)$ and/or the history of interaction force $F_h(t)$ at the device/fingertip interface. However, we did not use the amplitude of either x_h or F_h directly. Instead, we used the amplitude of the *commanded* sinusoidal vibration, which was a force amplitude (for these impedance-type devices). As described above, we called this the force commanded in software F_r, which was a sinusoid $F_r(t) = A_r \sin(2\pi f t)$. Thus the amplitude A_r was the primary independent variable (the parameter varied according to an adaptive scheme in search of the detection threshold). We assumed that the amplitude of the rendered force vibration $F_h(t)$ or displacement vibration $x_h(t)$ varied monotonically with the amplitude of the commanded force $F_r(t)$ for each participant. The relationship between the commanded signal $F_r(t)$ and the proximal stimulus $x_h(t)$ is of course a function of the device hardware and the impedance of the participant's grip, and the latter was experimentally deduced from accelerometer measurements post hoc. Accelerometer measurements were conducted for each experimentally determined smallest distinguishable proximal stimuli and for each subject individually. The relationship between the proximal stimulus and the participant's response is a function of human sensitivity. The spectral displacements of the smallest distinguishable proximal stimuli were estimated from the accelerometer measurements.

Per this method, the participant was presented with three randomly ordered stimuli. Two of them were generated by a null force command $F_r(t) = 0$ while the third was generated by the sinusoidal signal $F_r(t) = A_r \sin(2\pi f t)$. The participant used their nondominant hand on the computer keyboard to cycle through the three stimuli. They also used the keyboard to identify the one stimulus they judged as being different from the other two. There was no limit to either the number of times they could cycle through the triplets or the time they could spend observing any individual stimulus. The time that the participant spent with each stimulus varied from a brief dwell early in the experiment (when the task was easy) to more extended dwells later in the experiment (when the

1. Note that our experiment required well-trained participants who were able to maintain a consistent grip of the ball/stylus interface on the haptic devices. We did not recruit more participants because each participant had to be tested for several hours, and we were only interested in a within-participant comparison of device effects. It is however possible that there could have been an order effect due to the limited number of participants tested. This was probably unlikely as we observed similar patterns for each participant.

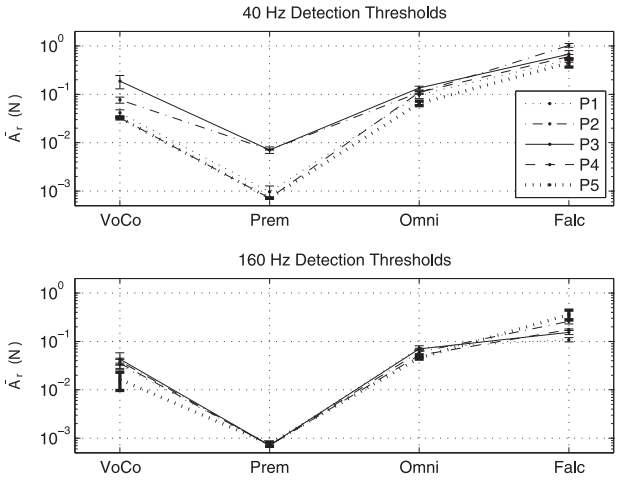

Fig. 2. $\bar{A}_r$ for the voice coil and three commercial haptic devices. VoCo—Voice Coil, Prem—Premium, and Falc—Falcon. (Modified from Fig. 2 in [1].)

task became harder) and also varied across participants and devices. There were no pauses between stimuli. To prevent temporal edge effects, transitions between stimuli were modified by an exponential function with 1 second rise and fall times. The initial stimulus amplitude was set for the null and test stimuli to be easily distinguishable by participants. Three consecutive correct responses resulted in a decrease in the amplitude of A_r. One incorrect response resulted in an increase of A_r. Modifications to the amplitude of A_r were 4 dB on the first 3 reversals, and 1 dB on the remaining 12 reversals, after which the test was over. Participants whose results did not converge were asked to repeat the experiment until convergence was obtained. Participants were tested at both frequencies on each device and took a break between experiments on each device. They were asked to report any comments they had about the experiment. A typical experiment for both frequencies on one device lasted 20 minutes.

2.1.4 Analysis of Position Threshold

For each device and each frequency, the last 12 reversals (six A_r peaks and six A_r valleys) were used to calculate the sinusoidal amplitude commanded in software $\bar{A}_r$ which resulted in the smallest proximal stimuli distinguishable from null stimuli by participants, and their standard deviations σ_A.

As mentioned earlier, we estimated the proximal vibration signal $x_h(t)$ from accelerometer measurements. We expressed the proximal stimulus in terms of $x_h(t)$ instead of $F_h(t)$ because most threshold data published in the literature are specified as vibration displacement. This was accomplished by commanding a sinusoidal force ($F_r(t) = \bar{A}_r \sin(2\pi f t)$) to the devices post hoc while the participant held the stylus or ball, and the accelerometer signal was recorded. A spectral analysis was undertaken on the accelerometer signal to deduce the spectral amplitudes and signal purity while raw temporal data were used to determine signal regularity.

From the literature, amplitude discrimination thresholds have been reported in the range 0.4-2.3 dB [26]. More specifically, our early study reported an amplitude discrimination threshold of 2.0-2.5 dB for stimuli in the frequency range 2-300 Hz under conditions similar to the present study [28]. For all practical purposes, we judge two signals of the same frequency to be perceived as similar if they differ in amplitude by less than 2.5 dB. When two signals of the same frequency differ in amplitude by more than 2.5 dB, then we judge them to be perceived as different since they can be reliably discriminated in a perception experiment.

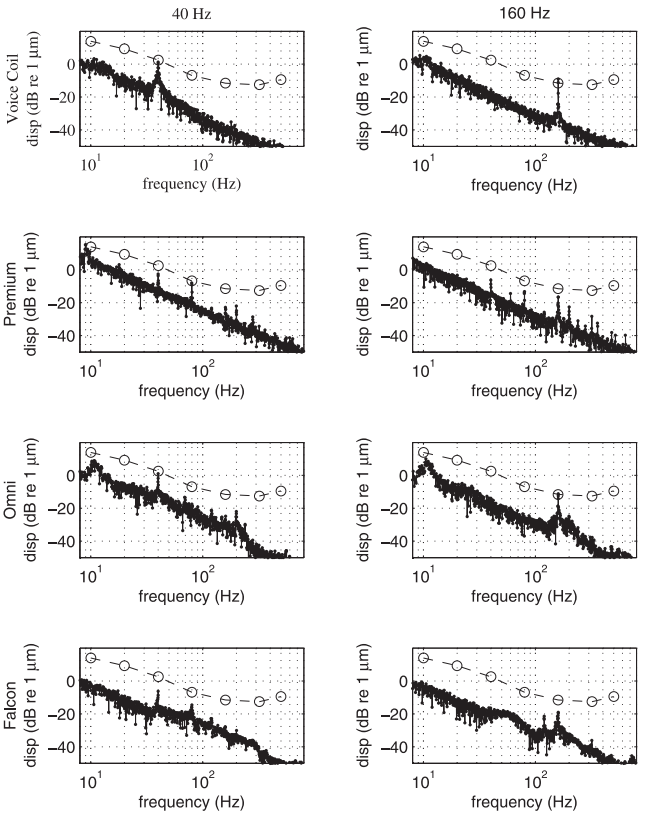

Fig. 3. Displacement spectra of the smallest distinguishable proximal stimuli for P1 for all devices and both frequencies. Columns are grouped by frequency tested and rows are grouped by device, as labeled. Dashed line segments connect threshold detection data (open circles) collected by Israr et al. [23]. (Modified from Fig. 3 in [1].)

2.2 Results

The smallest $\bar{A}_r$ which resulted in distinguishable proximal stimuli are shown in Fig. 2. The values of $\bar{A}_r$ were lower with the Premium than with the other two devices. Values of $\bar{A}_r$ for the Falcon are the highest, followed by the Omni and the Voice coil. There was a bimodal distribution in $\bar{A}_r$ with the Premium at 40 Hz. $\bar{A}_r$ for participants 2 and 3 (P2 and P3) were ≈ 10 mN while $\bar{A}_r$ for P1, P4, and P5 were $\bar{A}_r \approx 1$mN.

Fig. 3 contains the displacement spectra of the smallest distinguishable proximal stimuli. Again, the smallest distinguishable proximal stimuli were characterized by measuring the acceleration at the stylus while the participant (P1 in this case) held the stylus and while the haptic devices were sent sinusoidal forces commanded in software with amplitudes corresponding to $\bar{A}_r$. Spectral content at approximately 10 Hz is tremor induced by P1. We compared these spectra to the detection thresholds identified by Israr

et al. [23]. These authors measured displacement detection thresholds of vibrations with a high-fidelity minishaker actuator. Many more frequencies were tested in Israr et al., and we use those data to get a sense for which spectral components from our experiments are likely suprathreshold and which are likely subthreshold.

Averaged across participants, the amplitudes of the 40 Hz spectral displacement components of the proximal stimuli, resulting from commanding a 40 Hz sinusoid with the corresponding $\bar{A}_r$ amplitude in software, generated by the voice coil, Premium, Omni, and Falcon were 3.6 dB higher, 8.8, 2.7, and 5.4 dB lower, respectively, than detection thresholds identified by Israr et al. [23]. The amplitude of the 40 Hz component for P5 was particularly high (14.5 dB higher than thresholds identified by Israr et al.). Interestingly, this participant also had the lowest dwell times on any particular stimulus, which might have contributed to the high 40 Hz component. Amplitudes of the 160 Hz spectral displacement components of the proximal stimuli, resulting from commanding a 160 Hz sinusoid with the corresponding $\bar{A}_r$ amplitude in software, generated by the voice coil, Premium, Omni, and Falcon were 0.6, 13.0, 5.6, and 10.8 dB lower for our participants, respectively, than detection thresholds identified by Israr et al. We note that the order of sensitivity for the spectral displacement of the smallest distinguishable proximal stimuli is different than the order for $\bar{A}_r$. This inconsistency within participants is likely due to the different electrical and mechanical transfer functions for each device. The inconsistency across participants may be due to the firmness of the participants' grip.

The spectra for P1 show that the voice coil produced the most distortion-free signal for both frequencies, which held true across all participants. The commercial haptic devices produced significant harmonic distortion at both frequencies, which also held true across all participants. Most notable is the 40 Hz signal presented by the Premium to P1. The magnitude of the 80 Hz component was closer (2.4 dB lower) to the detection threshold identified by Israr et al. [23] than the 40 Hz fundamental (10.2 dB lower). This was also true for P4 and P5. While the data for P2 and P3 also exhibited significant distortion, only the 40 Hz signal was suprathreshold. With the Premium, the three participants reported a dramatic difference in the quality of the vibrations between clearly suprathreshold proximal stimuli and the smallest distinguishable proximal stimuli, meaning that they most likely perceived the 80 Hz harmonic component at low A_r and perceived the 40 Hz fundamental component at a higher A_r.

A sample of the temporal data collected for P3 is shown in Fig. 4. Inspection of the temporal data for the voice coil and Premium showed consistent periodicity with a fundamental frequency at the commanded frequency. The temporal data for the Omni and Falcon, however, showed aperiodic, sporadic responses, especially when driven by a 40 Hz signal.

2.3 Discussion

The amplitudes of the 160 Hz components of the proximal stimuli (resulting from commanding a 160 Hz sinusoid with the corresponding $\bar{A}_r$ amplitude in software) generated by the voice coil were similar to detection thresholds found in the published literature. The amplitudes of the 40 Hz components of the proximal stimuli, resulting from commanding a 40 Hz sinusoid with the corresponding $\bar{A}_r$ amplitude in software, generated by the voice coil were different from (higher than) the thresholds found in the literature, due to the outlier generated by P5. In contrast, the corresponding amplitudes of the 40 and 160 Hz components generated by the Premium, Omni, and Falcon were different from (lower than) the detection thresholds found in the literature. The smallest distinguishable proximal stimuli for the Premium were often dictated by harmonics rather than the fundamental frequency. Additionally, the displacement behavior of the Falcon and Omni was sporadic in both the spectral content and associated amplitudes. Here we discuss the electrical and mechanical causes of these results.

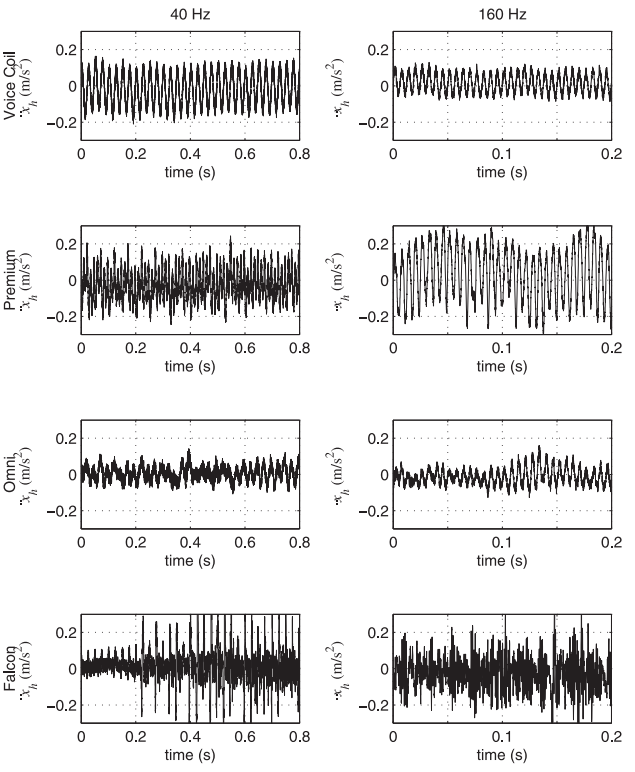

Fig. 4. Temporal traces of acceleration data of the smallest distinguishable proximal stimuli for P3 for all devices and both frequencies. Columns are grouped by frequency tested and rows are grouped by device, as labeled.

To fully describe the electrical and mechanical behavior of a haptic device, there are a significant number of attributes that must be characterized. Hayward and Astley provide a comprehensive list of these attributes [29]. We need to understand how these attributes affect the relationship between the commanded forces F_r and the forces rendered at the hand F_h. Furthermore, not all of the rendered forces will register force percepts F_p to the user. Understanding which forces are perceptible will aid in localizing the problem. In Fig. 5, we represent the signal flow through these electrical and mechanical modifiers that occurs during a haptic interaction.

Fig. 5 makes apparent that the commanded force F_r relates only in a distant sense to the perceived force F_p and displacement x_p. The original F_r signal passes through many

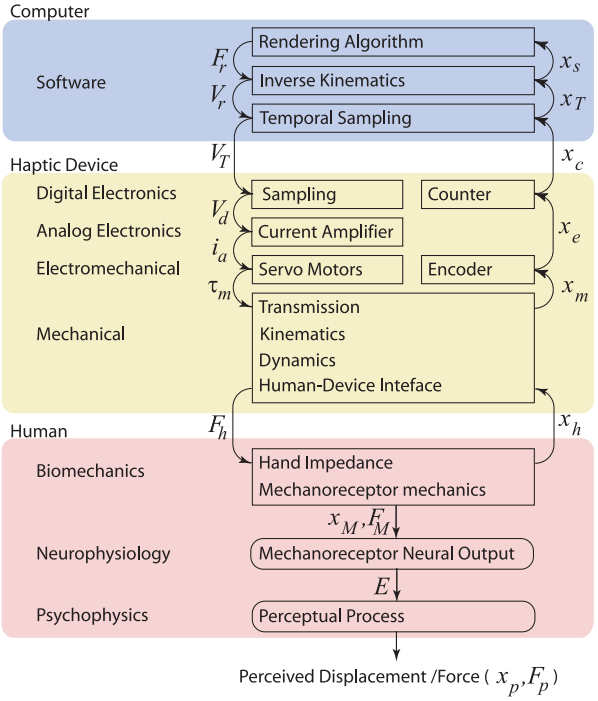

Fig. 5. Block diagram of signal flow from computer through haptic device to human and back. (Modified from Fig. 5 in [1].)

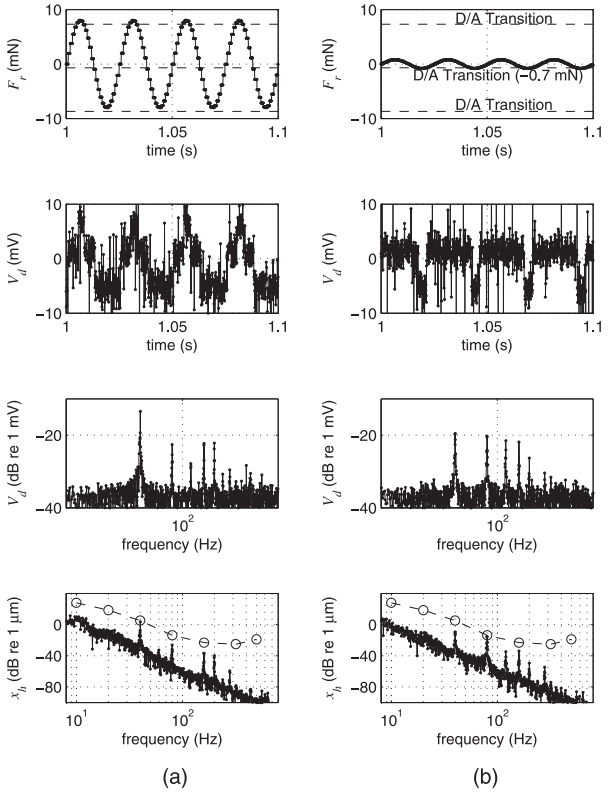

Fig. 6. D/A distortion data resulting from commanding the haptic devices with their corresponding $\bar{A}_r$ for 40 Hz for P1 and P2. (a) The data for P2 and (b) the data for P1. The top row shows the commanded force. The remaining rows show voltage from the D/A, the spectral content of this voltage, and the position spectrum at the stylus, respectively. (Modified from Fig. 6 in [1].)

electrical and mechanical modifiers, each of which can mask desired signal features and introduce undesired artifacts. The first modifier is a computational transformation involving the inverse kinematics and gain relating joint torques to reference voltages V_r. The next modifier involves the update rate of the haptic program (the virtual environment simulator) which samples V_r in time and applies a zero order hold, producing V_T. The output electronics then sample V_T in amplitude through the digital-to-analog converter. Both sampling processes can introduce signal distortion.

The resulting signal V_d then passes through the current amplifier and this current i_a is converted to torque τ_m through a servo motor. The amplifier can introduce deadband and delay while the motor may exhibit torque ripple. The torque passes through a transmission and the kinematics of a linkage and terminates at the human-device interface with an applied force F_h and its associated displacement x_h. All mechanical elements can exhibit backlash, stiction, viscous friction, elasticity, and can have inertia. The perceived force F_p and displacement x_p are the result of F_h and x_h being modified by physiological and psychophysical modifiers of the human, where x_M and F_M are the induced motions of the mechanoreceptors themselves and E is the action potential that is sent along the neurons from the mechanoreceptors to the brain. Because our experiments operated the haptic devices in open loop, we can ignore the position feedback signals which are shown on the right hand side of Fig. 5.

2.3.1 Digital Electronics Output Resolution

The resolution of the digital electronics output was identified as a primary source of distortion in the Premium. This was made clear by observing V_d, a signal which is accessible on the Premium by opening the amplifier box and measuring the reference voltage to the amplifiers with our NIDAQ board, described earlier. Fig. 6 shows the temporal and spectral data of V_d for the smallest distinguishable proximal stimuli for a 40 Hz commanded force for P1 and P2, along with the temporal data of F_r and the spectral data of x_h. As is evident from the temporal data of V_d, the resolution of the digital-to-analog converter is 5 mV which corresponds to an F_r of 8 mN when the stylus is in the home position. The dashed horizontal lines in the plots of F_r show the transition values of the D/A. Note that the D/A transition level closest to zero for our particular device is at $F_r = -0.7$ mN.

The $\bar{A}_r$ for 40 Hz for P2 and P3 found using the Premium results in a analog signal amplitude required from the D/A converter which is near the resolution of the D/A converter. This coarse quantization by the D/A created significant harmonic distortion. Many of the harmonics observed in the spectral plot of V_d are also present in the displacement spectral data x_h for P2 as shown in Fig. 6. Despite a resolution on F_r of 8 mN, the $\bar{A}_r$ for 40 Hz for P1, P4, and P5 with the Premium are an order of magnitude less than the D/A resolution. Inspection of the temporal and spectral data shown for P1 in Fig. 6 explains this phenomenon. Because the low amplitude F_r signal crosses a D/A transition, albeit only slightly, there is a jump from 0 to -5 mV on V_d. Furthermore, because F_r is not centered on the D/A transition for P1, the D/A signal has a duty cycle of about 25 percent. This becomes evident in the spectral plot of V_d for P1 by virtue of the lower 40 Hz component

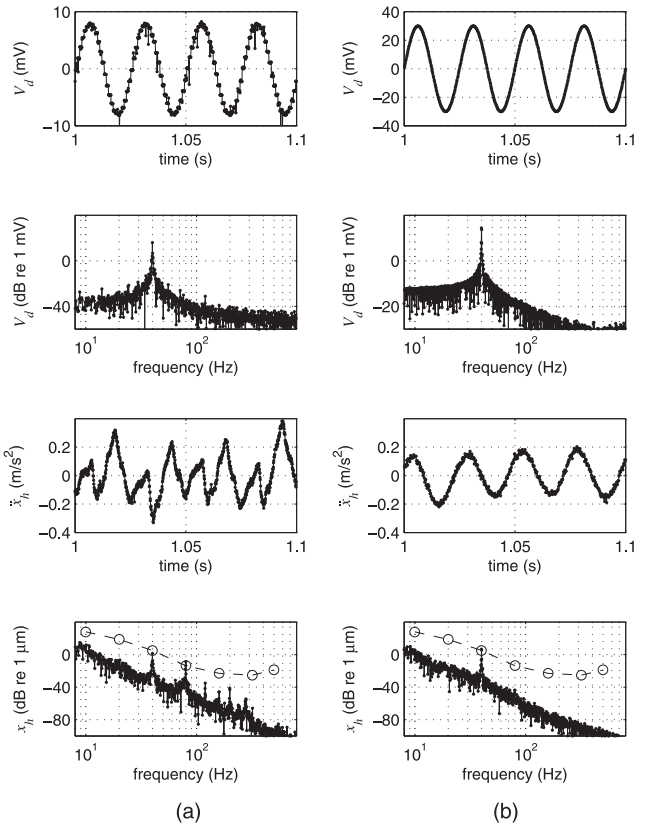

Fig. 7. Amplifier distortion data. (a) Data collected using the Premium amplifiers. (b) Data collected using high fidelity amplifiers. The top row shows the signal being sent to each amplifier. The remaining rows show the spectra of this voltage, the acceleration measured by the accelerometer at the stylus, and the displacement spectra, respectively. (Modified from Fig. 7 in [1].)

and higher 80 Hz component relative to the spectral data collected from P2. Furthermore, the spectral data for x_h show the 40 Hz component is subthreshold while the 80 Hz component is at the detection threshold identified by Israr et al. [23]. Consequently, those participants with a lower $\bar{A}_r$ at 40 Hz were instead cueing off the 80 Hz harmonic. Further reduction in the A_r would prevent the signal from crossing the transition value of -0.7 mN altogether and would result in an amplitude of x_h of zero. Consistent with this sharp drop in amplitude to zero, participants described a very noticeable distinction between the signals at levels they could perceive and at levels they could not. This was particularly true at 160 Hz. Evidently, all participants could perceive the lowest nonzero signal the D/A could transmit.

2.3.2 Amplifier Nonlinearities

Further investigation into the internal signals of the amplifier of the Premium showed that the amplifier exhibits crossover distortion. To isolate the distortion created by the amplifiers, we first sent a commanded force signal at 40 Hz with an amplitude near $\bar{A}_r$, but with a D/A resolution of 20 times the stock Premium D/A resolution. The 20x increase was accomplished with a 20x decrease in the gain setting on the Copley amplifiers. While this reduced the range of available force, it did not affect our experiments since they require only small forces. These data are shown in column (a) of Fig. 7.

We then bypassed the amplifier and directly commanded voltage to the Premium motors with the NIDAQ board. Again, the 5 mA drive capability of the NI boards was sufficient to drive the Premium directly for this experiment. These data are shown in column (b) of Fig. 7 for comparison. Any discrepancies in $\ddot{x}_h$ and x_h spectra between the two data sets can be attributed exclusively to the amplifier. We point out that there is a noticeable difference between the data. The harmonic distortion created by the Premium amplifiers is suprathreshold whereas such distortion is not present when the amplifier is removed.

The amplifiers in the Premium we used are 300 series Copley Amplifiers (Copley Controls Corp, Canton, MA). These amplifiers use a drive-brake PWM scheme to modulate current output. This PWM scheme modifies the duty cycle on a square wave whose rails are at 0 and 30 V in the forward direction. In order to reverse the current direction, there is a switch that enables the PWM rails to change to 30 and 0 V, respectively. This transition has hysteresis, drift, and time delay. This behavior contributes to harmonics observed in the accelerometer data. In contrast, both the Falcon and Omni operate on a locked antiphase scheme in which the rails are at ± 30 and ± 18V, respectively. Consequently, the deleterious behavior is not exhibited by these devices.

2.3.3 Stiction

Inspection of the accelerometer data for both the Falcon and the Omni show that stiction plays a dominant role in signal regularity and the associated presence of harmonics.

To quantify the stiction and its effect on the presentation of sinusoidal signals, we commanded each device with a 40 Hz signal (F_r) whose amplitude ramped up and then down as a linear function of time. We repeated the test with a 160 Hz signal. The acceleration was measured while participant P1 held the stylus. Fig. 8 shows the results of the 40 Hz test on the Falcon and Omni.

From the subfigures on the left of Fig. 8, which describe the behavior of the Falcon, we can deduce that the stiction is broken on the ramp up when the amplitude of F_r exceeds 0.84 N (0.48 N at 160 Hz). On the ramp down, the amplitude at which the stiction fully re-engages is 0.61 N (0.31 N at 160 Hz). For the Omni the stiction is shown to be broken at 0.099 and 0.12 N on the ramp up for 40 and 160 Hz, respectively, and 0.079 and 0.10 N on the ramp down. These F_r values are consistent with the $\bar{A}_r$ values obtained with the Falcon and Omni. The plots at the second and fourth row for the Falcon and Omni of Fig. 8 show a more narrow time window centered about the break point for stiction. Notice that even when the commanded amplitude is high enough to break the stiction, the stiction still re-engages at every peak and valley of the force and acceleration profiles. In these instances the velocity is zero and the stiction can re-engage. The disengagement and re-engagement of stiction, amplified by the device dynamics, is the primary source of the harmonics observed on both the Falcon and the Omni. The sporadic response seen in the time domain is caused by the device disengaging and re-engaging stiction over time. Participant-induced motion was observed to occasionally break the stiction, thereby reducing the amplitude of F_r required to break the stiction.

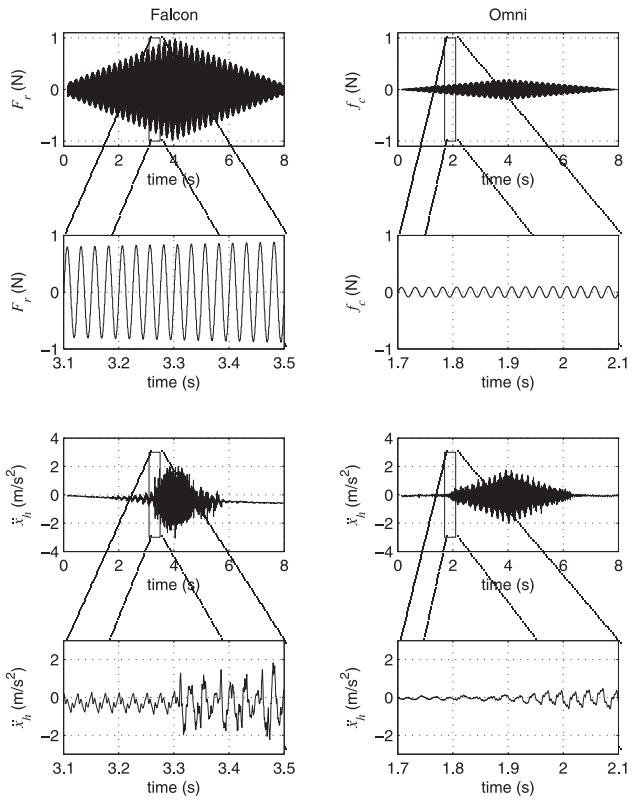

Fig. 8. Ramp up and down amplitude on 40 Hz commanded force. The left column contains the data collected with the Falcon and the right column contains the data collected with the Omni. The top row is the commanded force sent to each device. The third row is the acceleration measured at the human-device interface of each device. Second and fourth row plots show a smaller time window of the same data shown in the corresponding plots immediately above them.

3 Experiment 2

An implication of our findings in experiment 1 is that the Premium would be "good enough" if its D/A resolution and amplifier linearity were improved. Furthermore, the Falcon and Omni would be "good enough" if their static friction were reduced. In this second experiment, we attempt to make or simulate these hardware improvements and then rerun the experiments on the same participants.

3.1 Method

3.1.1 Apparatus

The gain of the Copley amplifiers of the Premium are set by two external resistors. In order to increase the effective resolution of the D/A, we decreased the gain by a factor of 20. While this reduced the range of force, it did not prevent the haptic device from producing distinguishable proximal stimuli, the smallest of which require only small forces. To reduce the crossover distortion of the Premium amplifier, a DC offset was added to the sinusoidal commanded force signal. This prevented the amplifier signal from operating the current-direction switch which caused the crossover distortion. This offset was compensated for by the participants with the application of a supporting reaction force. The offset was reduced as the sinusoidal amplitude was reduced to minimize the effects of DC load on perception. All other apparatus parameters were identical to those in experiment 1.

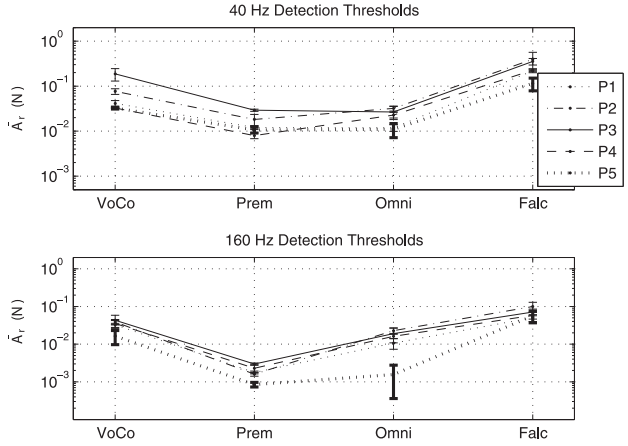

Fig. 9. $\bar{A}_r$ for the voice coil and three commercial haptic devices.

3.1.2 Participants

The same five participants from experiment 1 participated in this experiment to facilitate within-participant comparisons.

3.1.3 Procedure

The stiction of both the Omni and the Falcon were overcome by requiring the participants to move the stylus forwards and backwards in the vibration direction while undergoing the experiment. Because no changes were made to the voice coil, experiments were not rerun on this device. All other procedures were identical to those of experiment 1.

3.2 Results

The smallest $\bar{A}_r$ which resulted in distinguishable proximal stimuli are presented in Fig. 9. The values of $\bar{A}_r$ with the Premium are larger for all participants at both frequencies than in experiment 1. The values of $\bar{A}_r$ with both the Omni and the Falcon are smaller for all participants at both frequencies than in experiment 1. Values of $\bar{A}_r$ were quite similar between the Premium and Omni at 40 Hz. Values of $\bar{A}_r$ were quite similar between the voice coil and Omni at 160 Hz. P5 had a noticeably lower $\bar{A}_r$ than other participants on both the Premium and the Omni.

Fig. 10 contains the displacement spectra determined from the accelerometer measurements for P1. We again compared these spectra to the detection thresholds identified by Israr et al. [23]. Averaged across participants, the amplitudes of the 40 Hz spectral displacement components of the proximal stimuli (resulting from commanding a 40 Hz sinusoid with the corresponding $\bar{A}_r$ amplitude in software) generated by the voice coil, Premium, Omni, and Falcon were 3.6, 2.4, 4.7, and 2.8 dB higher, respectively, than detection thresholds identified by Israr et al. [23]. Amplitudes of the 160 Hz spectral displacement components of the proximal stimuli (resulting from commanding a 160 Hz sinusoid with the corresponding $\bar{A}_r$ amplitude in software) generated by the voice coil, Premium, Omni, and Falcon were 0.6, 14.5, 1.6, and 2.7 dB lower, respectively, than detection thresholds identified by Israr et al. When adjusted by the individual detection thresholds estimated using the voice coil, the amplitudes at 40 Hz for the Premium, Omni, and Falcon are 1.2 dB lower, 1.1 dB higher, and 0.8 dB lower, respectively. Likewise, the amplitudes at

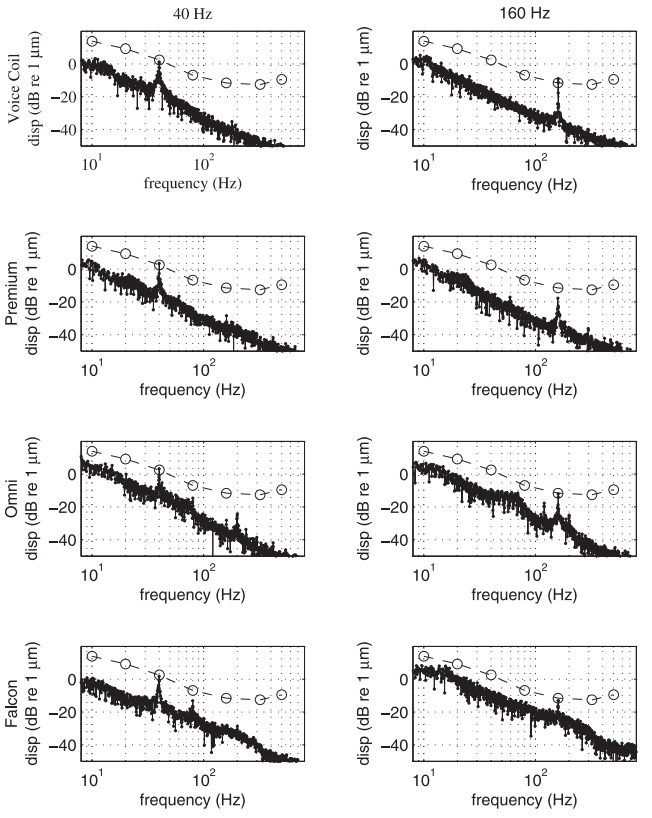

Fig. 10. Displacement spectra of the smallest distinguishable proximal stimuli for P1 for all devices and both frequencies. The left column is the data for the 40 Hz condition. The right column is the data for the 160 Hz condition. The rows are grouped by device. From top to bottom is the voice coil, Premium, Omni, and Falcon. Dashed line segments connect threshold detection data (open circles) collected by Israr et al. [23].

160 Hz for the Premium, Omni, and Falcon are 13.9, 1.0, and 2.1 dB lower, respectively.

The spectra for P1 show that the harmonic distortion was significantly reduced for all three of the commercial haptic devices, a fact that held true across all participants. The small amount of subthreshold harmonic distortion still present in the Omni and Falcon are attributable to the inability to entirely remove the effect of stiction by cyclically moving the device stylus. Inspection of the temporal data revealed signals with much more regular, periodic behavior. Fig. 11 shows a sample of the temporal data collected with P4. The traces for the Omni and Falcon show the back and forth motion produced by the participant to break the stiction. To the extent that the stiction is broken in these plots, the acceleration data are more periodically regular than in experiment 1.

3.3 Discussion

In this experiment, we showed that minor hardware and procedural modifications were sufficient to overcome the dominant hardware limitations discovered in experiment 1. Having participants actively, albeit slowly, move the interface of the Omni and Falcon improved the regularity and periodicity of the vibration signal, as well as facilitated the presence of only one perceptible spectral component (at the commanded frequency) in the proximal stimulus whose amplitude was similar to that estimated with the voice coil. As a result, we found no adverse effects of this active

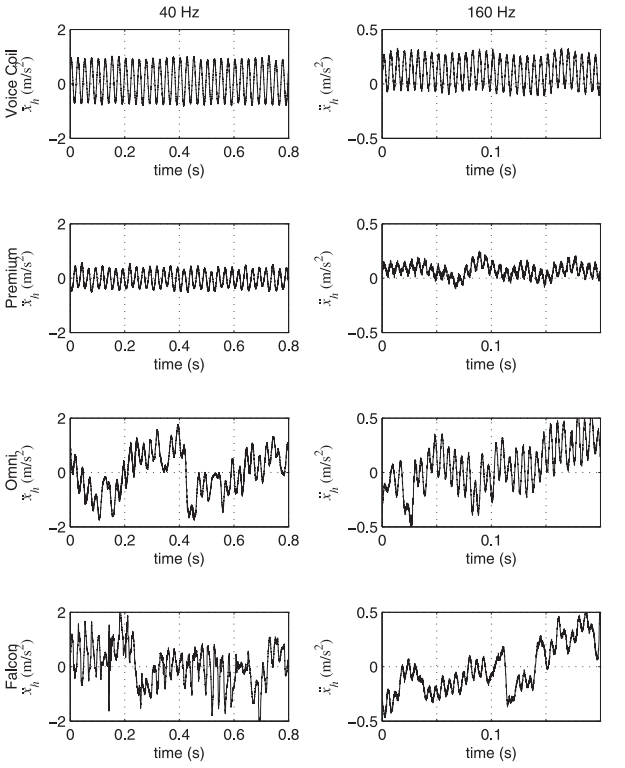

Fig. 11. Acceleration data of the smallest distinguishable proximal stimuli for P4 for all devices and both frequencies. The left column is the data for the 40 Hz condition. The right column is the data for the 160 Hz condition. The rows are grouped by device. From top to bottom is the voice coil, Premium, Omni, and Falcon.

motion. The adjustments made to the Premium resulted in only the 40 Hz component being perceptible when the device was commanded at 40 Hz, and the displacement amplitude of the 40 Hz component was similar to that estimated with the voice coil and the detection threshold found in the published literature. When these limitations were overcome, however, new issues became apparent. Based upon our measurements of the smallest proximal stimuli that participants claimed to be capable of distinguishing, the amplitudes of all the spectral components appeared to be significantly lower than detection thresholds. Furthermore, P5 had an exceptionally low $\bar{A}_r$ at 160 Hz on the Omni. Here we investigate the causes of the findings.

3.3.1 Directional Crosstalk

Directional crosstalk caused by mechanical coupling of oscillations from one direction to the other two orthogonal directions was the primary cause for the spectral content of the smallest distinguishable proximal stimuli (generated by commanding a 160 Hz force sinusoid in software to the Premium) to appear well below detection thresholds. This was made clear by measuring the acceleration in three orthogonal directions at the stylus while vibrations were commanded in only the X direction (see Fig. 12) The accelerometer we used (model ADXL330, 300 mV/g, 0.5-550 Hz, SparkFun Electronics, Boulder, CO) provided good sensitivity to low values of acceleration and weighed only 2 grams.

It is clear from Fig. 12 that a significant amount of motion is generated in directions other than the commanded

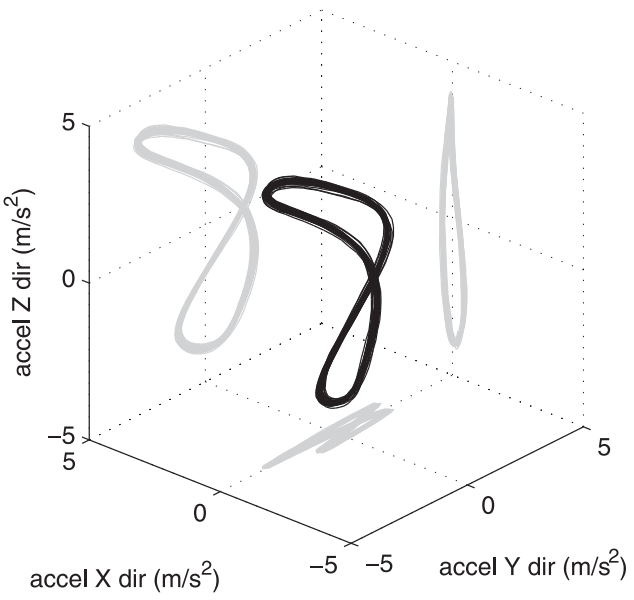

Fig. 12. 3D acceleration data at Premium stylus while vibration commanded in X direction.

X direction. Acceleration is greater by a factor of nearly 10 in the Z direction and over 5 in the Y direction compared to the X direction. At 160 Hz, the operating mechanoreceptors are the Pacinian corpuscles. These mechanoreceptors do not resolve vibrational direction [30]. Consequently, perceptual reporting of vibration stimuli is likely based upon the maximum displacements rather than the displacements in the X direction alone. The accelerometers we used in Fig. 10, however, were single axis and only measured vibration in the X direction. Likely for this reason, the amplitudes of the 160 Hz component in particular appeared to be lower with the Premium at 160 Hz, but they were in fact very similar to the amplitudes identified with the other devices at 160 Hz.

3.3.2 Digital Electronics Output Resolution

Participant P5 showed a lower $\bar{A}_r$ on the Omni for the same reason participants had a lower $\bar{A}_r$ on the Premium in the previous experiment—the signals being sent to the Omni were below the D/A resolution. This was not evident in experiment 1 because the stiction of the Omni dominated the smallest distinguishable proximal stimuli. Even though the signals sent to the D/A were decreasing, the output of the D/A remained constant. The transition level nearest zero on the Omni was crossed at approximately 0.2 mN. As a result, the shift in duty cycle at the D/A output that was observed with the Premium was not observed with the Omni. Rather, as the commanded force amplitude decreased, the 160 Hz signal persisted at a full 8 mN amplitude until the signal no longer crossed the D/A transition level, at which point the D/A output was zero.

4 Psychophysically Informed Design Limits and Recommendations

While we attempted to significantly remove harmonic distortion in our second experiment, of interest is the amount of harmonic distortion a device can present without being detected by the human user. Bensmaia et al. showed that Pacinian-based vibratory perception was well characterized by a pattern of activation in a set of frequency-tuned minichannels [31]. Their conclusions suggest that an arbitrary signal is detectable if one or more of its spectral components has a suprathreshold amplitude. The work of Cholewiak and Tan also supports this conclusion [6]. They observed that detection amplitudes of square wave signals could be predicted by the detection amplitude of a sine wave signal representing the first (and largest) Fourier component of the square wave signal.

Our work also supports the conclusion that an arbitrary signal is distinguishable from a null stimulus if one or more of its spectral components has a suprathreshold amplitude [31]. In Fig. 3, the 40 Hz signal presented by the voice coil to P1 is detectable because the 40 Hz component is suprathreshold. The 40 Hz signal presented by the Premium, on the other hand, is detectable because the 80 Hz component generated by signal distortion is suprathreshold.

From this we draw the very useful conclusion that signal distortion is acceptable so long as all of the distortion components have subthreshold amplitudes. More specifically, a device designer must keep the effects of finite D/A resolution, amplifier distortion, stiction, and any noise sources low enough that, once propagated through the system dynamics, the motions are subthreshold. Because detection thresholds for humans are both consistent and well characterized, quantitative design guidelines can be derived from this approach. We will elaborate on this by example in the next sections.

4.1 Actuator Resolution

The signal distortion generated by the D/A resolution can be approximated by the spectral content of a square wave with an amplitude of a single D/A tick and a frequency equal to the lowest commanded frequency. As such, the amplitude of the harmonics of a quantized commanded signal will generally not exceed 1/3 the resolution of the D/A. A conservative envelope of the noise would be a white noise with an amplitude of a single D/A tick. When specifying the D/A resolution, the designer would need to ensure that this level of white noise, after passing through the system dynamics, is subthreshold.

As an example we consider the Premium. We characterized the transfer function of the device when the stylus is held by P1. We did this by averaging multiple sine sweeps up and down in frequency and with a commanded force sinusoid of 0.1 N in the X direction. Fig. 13 shows the Premium displacements as a function of frequency for four different sweep commanded amplitudes. These displacements were calculated by scaling the transfer function by the commanded force. Because a commanded force in the X direction excites motions in all directions, the displacements shown in Fig. 13 represent the maximum displacement of the three orthogonal directions for each frequency. It is clear that all signals of any frequency that are below 1 mN will not be perceptible. This is supported by our experiments which show that the standard resolution on the Premium of 8 mN causes perceptible harmonics. Furthermore, when the resolution was reduced to 0.4 mN, no such harmonics were perceived. We recommend a D/A resolution of 1 mN for the Premium haptic device. Using a similar method, the recommended resolution for the Omni and Falcon are 1 mN and 10 mN, respectively. We note that the current off the shelf native resolution of these devices is 7 and 25 mN, respectively.

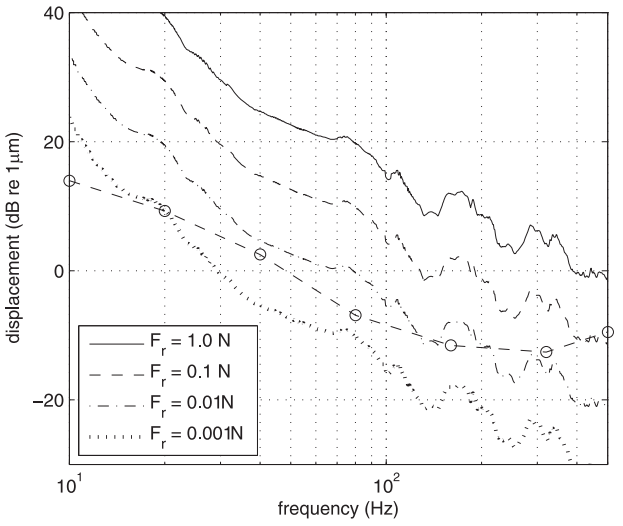

Fig. 13. Premium spectral output for four sweep commanded amplitudes compared to detection thresholds.

4.2 Amplifier Nonlinearities

The detectable nonlinearities generated by the current amplifiers can be minimized by using a locked antiphase PWM scheme. Because locked antiphase PWM technology is pervasive and inexpensive, its use is recommended in all haptic applications.

4.3 Device Stiction

We have observed motor stiction to be the primary source of device stiction in haptic hardware. This feature, which is perhaps of unique interest to the haptic community, is not always published by vendors in data sheets. This attribute must therefore be measured on candidate motors. In general, the stiction needs to be low enough such that, once broken, the stylus displacements are subthreshold. The stiction in the Falcon, for example, would need to be reduced by nearly an order of magnitude to meet this criterion.

4.4 Directional Crosstalk

Directional crosstalk is perhaps the most difficult hardware attribute to eliminate through a design modification. Rotational joints pervade the kinematic design for haptic devices due to their many attractive features. Inherent in linked rotational joints, however, is directional coupling of motor efforts and directional motions. This coupling, which exists in static loading conditions, can be exacerbated in dynamic loading conditions. We recommend characterizing this feature of the device and scaling the commanded force accordingly.

5 Concluding Remarks

We have shown that the concept of CSF can be applied to human-plus-device evaluation of haptic devices using vibration detection experiments. In particular, vibration detection experiments were shown to be an effective way to measure the suitability of a haptic device for rendering the vibratory components of texture. Interestingly, we found that the distinguishable spectral components of a proximal stimulus were not always of the same frequency as the force sinusoid commanded in software. In some cases, the distinguishable signals were harmonics. As far as we are aware, the literature on visual CSF as it relates to the evaluation of the "eye-plus-instrument" system never discussed the effects of harmonics, possibly due to the different ways the human visual and haptic sensitivity curves are shaped (i.e., people are more sensitive to lower frequency visual gratings than to higher frequency ones; see [32]). Our finding points to the importance of not only conducting quantitative measurements of HCSF but paying attention to the qualitative changes in haptic vibratory signals.

Our first set of experiments found deficiencies with regard to rendering the vibratory component of texture in three commercial haptic devices. Vibration detection experiments were also shown to be valuable tools for identifying the limiting device factors in the ability of these three haptic devices to be "good enough" at rendering the vibratory component of texture. We identified these factors to be digital electronics output resolution, amplifier nonlinearities, and stiction. By improving these factors we showed that the devices were then capable of presenting spectrally clean signals at human detection thresholds. Finally, these experiments facilitated the development of quantitative design guidelines for ensuring the suitability of a haptic device for rendering the vibratory components of texture. For these reasons, we find vibration detection experiments to be a very powerful tool for the evaluation of haptic devices. While it is not exhaustive in its ability to evaluate haptic hardware, its ability to quantitatively evaluate the performance and guide the design of a number of hardware attributes makes its incorporation into any evaluation testbed attractive. Future work will look for other human-plus-device evaluations which, when coupled with the vibration detection experiment outlined in this paper, will comprise a full evaluation of the haptic hardware.

Acknowledgments

The first author was supported in part by Sandia National Laboratories. Portions of this article reprinted with permission from [1], ©2009 IEEE.

References

[1] C. Salisbury, R. Gillespie, H. Tan, F. Barbagli, and J. Salisbury, "Effects of Haptic Device Attributes on Vibration Detection Thresholds," *World Haptics Conf. (WHC '09): Proc. Third Joint EuroHaptics Conf. and Symp. Haptic Interfaces for Virtual Environment and Teleoperator Systems,* pp. 115-120, 2009.

[2] P. Mouroulis, "Contrast Sensitivity in the Assessment of Visual Instruments," *Assessment of Imaging Systems: Visible and Infrared SPIE*, vol. 274, pp. 202-210, 1981.

[3] C. Chen, G. Chiu, and J. Allebach, "Banding Reduction in Electrophotographic Process Using Human Contrast Sensitivity Function Shaped Photoreceptor Velocity Control," *J. Imaging Science and Technology,* vol. 47, pp. 209-223, 2003.

[4] S.J. Bolanowski Jr, G.A. Gescheider, R.T. Verrillo, and C.M. Checkosky, "Four Channels Mediate the Mechanical Aspects of Touch," *J. Acoustical Soc. of Am.,* vol. 84, pp. 1680-1694, 1988.

[5] K.O. Johnson, T. Yoshioka, and F. Vega-Bermudez, "Tactile Functions of Mechanoreceptive Afferents Innervating the Hand," *J. Clinical Neurophysiology,* vol. 17, pp. 539-558, 2000.

[6] S. Cholewiak, K. Kim, H. Tan, and B. Adelstein, "A Frequency-Domain Analysis of Haptic Gratings," *IEEE Trans. Haptics,* vol. 3, no. 1, pp. 3-14, Jan.-Mar. 2010.

[7] S.J. Lederman, J.M. Loomis, and D.A. Williams, "The Role of Vibration in the Tactual Perception of Roughness," *Perception and Psychophysics,* vol. 32, pp. 109-116, 1982.

[8] R.H. LaMotte and M.A. Srinivasan, "Surface Microgeometry: Tactile Perception and Neural Encoding," *Information Processing in the Somatosensory System*, O. Franzen and J. Westman, eds., pp. 49-58, MacMillan Press, 1991.
[9] K.O. Johnson and S.S. Hsiao, "Neural Mechanisms of Tactual Form and Texture Perception," *Ann. Rev. of Neuroscience,* vol. 15, pp. 227-250, 1992.
[10] K.O. Johnson and S.S. Hsiao, "Evaluation of the Relative Roles of Slowly and Rapidly Adapting Afferent Fibres in Roughness Perception," *Canadian J. Physiology and Pharmacology,* vol. 72, pp. 488-497, 1994.
[11] S.J. Lederman, H.R.L. Klatzky, C.L. Hamilton, and G.I. Ramsay, "Perceiving Roughness via a Rigid Probe: Psychophysical Effects of Exploration Speed and Mode of Touch," *Haptics-e: The Electronic J. Haptics Research,* vol. 1, pp. 1-20, 1999.
[12] R.L. Klatzky and S.J. Lederman, "Tactile Roughness Perception with a Rigid Link Interposed between Skin and Surface," *Perception and Pyschophysics,* vol. 61, no. 4, pp. 591-607, 1999.
[13] M. Hollins and S.R. Risner, "Evidence for the Duplex Theory of Tactile Texture Perception," *Perception and Psychophysics,* vol. 62, pp. 695-705, 2000.
[14] R. Klatzky and S. Lederman, "Perceiving Texture through a Probe," *Touch in Virtual Environments,* M.L. McLaughlin, J.P. Hespanha, and G.S. Sukhatme, eds., ch. 10, pp. 180-193, Prentice Hall PTR, 2002.
[15] D. Katz, *The World of Touch.* Lawrence Erlbaum Associates, 1925/1989.
[16] K. MacLean, "Emulation of Haptic Feedback for Manual Interfaces," PhD thesis, Dept. of Mechanical Eng., Massachusetts Inst. of Technology, 1996.
[17] D.A. Lawrence, L.Y. Pao, A.M. Dougherty, M.A. Salada, and Y. Pavlou, "Rate-Hardness: A New Performance Metric for Haptic Interface," *IEEE Trans. Robotics and Automation,* vol. 16, no. 4, pp. 357-371, Aug. 2000.
[18] M. O'Malley and M. Goldfarb, "The Effect of Force Saturation on the Haptic Perception of Detail," *IEEE Trans. Mechatronics,* vol. 7, no. 3, pp. 280-288, Sept. 2002.
[19] S. Choi and H. Tan, "Perceived Instability of Virtual Haptic Texture. I. Experimental Studies," *Presence,* vol. 13, no. 4, pp. 395-415, 2004.
[20] S. Choi and H. Tan, "Perceived Instability of Virtual Haptic Texture. II. Effect of Collision-Detection Algorithm," *Presence,* vol. 14, no. 4, pp. 463-481, 2005.
[21] S. Choi and H. Tan, "Perceived Instability of Virtual Haptic Texture. III. Effect of Update Rate," *Presence,* vol. 16, no. 3, pp. 56-60, 2007.
[22] G. Campion and V. Hayward, "Fundamental Limits in the Rendering of Virtual Haptic Interfaces," *Proc. First Joint Euro-Haptics Conf. and Symp. Haptic Interfaces for Virtual Environment and Teleoperator Systems (WHC '05),* pp. 263-270, 2005.
[23] A. Israr, S. Choi, and H. Tan, "Detection Threshold and Mechanical Impedance of the Hand in a Pen-Hold Posture," *Proc. IEEE/RSJ Int'l Conf. Intelligent Robotics and Systems,* pp. 472-477, 2006.
[24] http://www.chai3d.com, 2009.
[25] A. Israr, S. Choi, and H. Tan, "Mechanical Impedance of the Hand Holding a Sperical Tool at Threshold and Suprathreshold Stimulation Levels," *Proc. Second Joint EuroHaptics Conf. and Symp. Haptic Interfaces for Virtual Environment and Teleoperator Systems (WHC '07),* pp. 56-60, 2007.
[26] R.T. Verrillo and G.A. Gescheider, "Perception via the Sense of Touch," *Tactile Aids for the Hearing Impaired,* I.R. Summers, eds., ch. 1, pp. 1-36, Whurr Publishers, 1992.
[27] H. Levitt, "Transformed Up-Down Methods in Psychoacoustics," *The J. Acoustical Soc. Am.,* vol. 49, pp. 467-477, 1971.
[28] A. Israr, H.Z. Tan, and C.M. Reed, "Frequency and Amplitude Discrimination along the Kinesthetic-Cutaneous Continuum in the Presence of Masking Stimuli," *J. the Acoustical Soc. of Am.,* vol. 120, no. 5, pp. 2789-2800, 2006.
[29] V. Hayward and O. Astley, "Performance Measures for Haptic Interfaces," *Proc. Robotics Research: The Seventh Int'l Symp.,* pp. 195-207, 1996.
[30] W.R. Loewenstein and M. Mendelson, "Components of Receptor Adaptation in a Pacinian Corpuscle," *J. Physiology,* vol. 177, pp. 377-397, 1965.
[31] S. Bensmaia, M. Hollins, and J. Yau, "Vibrotactile Intensity and Frequency Information in the Pacinian System: A Psychophysical Model," *Perception and Psychophysics,* vol. 67, no. 5, pp. 828-841, 2005.
[32] F. Campbell and J.G. Robson, "Application of Fourier Analysis to the Visibility of Gratings," *J. Physiology,* vol. 197, pp. 551-566, 1968.

Curt M. Salisbury received the BS degree in mechanical engineering from Brigham Young University in 2001, the MS degree in mechanical engineering from the University of Washington in 2003, and the PhD degree in mechanical engineering from Stanford University in 2009. He is currently with the Intelligent Systems, Robotics and Controls Group at Sandia National Laboratories, Albuquerque, NM. His current research interests include haptic interface design, human motor behavior, prosthetics, and robotic hands.

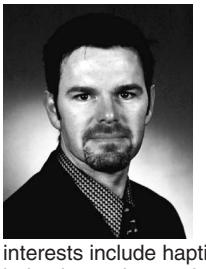

R. Brent Gillespie (M'97) received the BS degree in mechanical engineering from the University of California, Davis, in 1986, the MM degree in piano performance from the San Francisco Conservatory of Music in 1989, and the MS and PhD degrees in mechanical engineering from Stanford University in 1992 and 1996, respectively. He is currently with the Department of Mechanical Engineering, University of Michigan, Ann Arbor. His current research interests include haptic interface and teleoperator control, human motor behavior, robot-assisted rehabilitation after neurological injury, and prosthetics. He is a member of the IEEE.

Hong Z. Tan received the bachelor's degree in biomedical engineering from Shanghai Jiao Tong University in 1986 and the master's and doctorate degrees in 1988 and 1996, respectively, both in electrical engineering and computer science, from the Massachusetts Institute of Technology (MIT). She was a research scientist at the MIT Media Lab from 1996 to 1998 before joining the faculty at Purdue University. She is currently an associate professor of electrical and computer engineering, with courtesy appointments in the school of mechanical engineering and the department of psychological sciences. She is an associate editor of *Presence*, *ACM Transactions on Applied Perception*, *and IEEE Transactions on Haptics*. She served as the founding chair of the IEEE Technical Committee on Haptics from 2006-2008. She was a recipient of the National Science Foundation (NSF) CAREER award from 2000-2004. Her research focuses on haptic human-machine interfaces in the areas of haptic perception, rendering, and multimodal performance. She is a senior member of the IEEE.

Federico Barbagli received the PhD degree from Scuola Superiore S. Anna, Pisa, in 2002. He was a post doctoral fellow at the Stanford Robotics lab from 2002 to 2005, an assistant professor at the University of Siena from 2002 to 2004. In 2004, he joined Hansen Medical, a surgical robotic startup in Palo Alto CA. He served in various roles including senior fellow and CTO. He's currently a consulting associate professor at Stanford Computer Science and serves as technical advisor to various medical robotics companies.

J. Kenneth Salisbury received the PhD degree in mechanical engineering from Stanford. He is a professor in the computer science and surgery departments at Stanford. His research interests include humanmachine interaction, collaborative computermediated haptics, and surgical simulation. He is a member of the IEEE.